

The 9.2 ka event during the early Holocene recorded by a stalagmite from Dongge Cave

Chuntong He^{a,1}, Bin Zhao^{a,1}, Yongjin Wang^a, Kan Zhao^a, Shaohua Yang^b, Qingfeng Shao^a, Hai Cheng^c, Yijia Liang^{a,d,*}

^a School of Geography, Nanjing Normal University, Nanjing 210023, China

^b College of Economy and Management, Nanjing Vocational University of Industry Technology, Nanjing 210023, China

^c Institute of Global Environmental Change, Xi'an Jiaotong University, Xi'an 710054, China

^d School of Geographical Science, Nantong University, Nantong 246000, China

ARTICLE INFO

Editor: Dr. Pradeep Srivastava

Keywords:

Asian monsoon
Stable isotopes
Dongge Cave
The 9.2 ka event
Holocene

ABSTRACT

It is important to understand the variability and mechanisms of the Asian summer monsoon during the Holocene, yet the dynamics of the Asian monsoon weakening in response to the 9.2 ka event remain controversial. We reconstructed paleoclimate records with 12 $^{230}\text{Th}/\text{U}$ dates and 199 pairs of $\delta^{13}\text{C}$ and $\delta^{18}\text{O}$ from a stalagmite in Dongge Cave, southwestern China, covering from ~2332 to 9793 a BP. Our records provide new evidence for interpreting centennial-scale monsoon variabilities and environmental changes during the early Holocene. Our sample sensitively captures the 8.2 and 9.2 ka events, exhibiting significantly positive isotopic shifts. Of note is the $\delta^{13}\text{C}$ record, which displays dramatic oscillations during these events, reflecting the rapid response of terrestrial ecosystems and vegetation to abrupt climate changes. Comparison with other geological records suggests that the cause for the 9.2 ka event differs from the 8.2 ka event, the latter of which was dominantly forced by iceberg collapse and freshwater input in the North Atlantic. However, the 9.2 ka event may have been affected by the synergistic effect of solar activity and the Atlantic Meridional Overturning Circulation, which leads to a southward shift of the Intertropical Convergence Zone and triggers sudden changes in the Asian summer monsoon.

1. Introduction

The Asian monsoon is an important atmospheric circulation within the global climate system. It bridges the high northern latitudes and the tropics, and plays a significant role in the global hydrological and energy cycles (Ding and Chan, 2005). Understanding the nature of Asian monsoon variability and its forcing mechanisms is essential for contextualizing current environmental and hydroclimatic conditions, and for effectively predicting climate change under scenarios of future global warming (Wang et al., 2013; Ding and Chan, 2005).

The Holocene climate is marked by a series of abrupt centennial-scale climate oscillations (You et al., 2025; Zhang et al., 2025; McKay et al., 2024; Wang et al., 2023; He et al., 2022). And a large body of evidence suggests that the early Holocene, considered relatively stable, also experienced abrupt climate changes (Kobashi et al., 2017; Dykoski et al., 2005; Bond et al., 1997). The most notable rapid climate change

occurred at around 8.2 ka BP (the 8.2 ka event), a global climate anomaly that has received significant attention and has been studied in many regions of the world, including Greenland, the North Atlantic, the Mediterranean, Asia, East Africa, North America, and Antarctica (Zhang et al., 2025; McKay et al., 2024; Wood et al., 2023; Fleitmann et al., 2007; Fleitmann et al., 2003; Alley and Agustsdottir, 2005; Johnsen et al., 2001; Barber et al., 1999; Alley et al., 1997; Stager and Mayewski, 1997). The impact of the 8.2 ka event on the Asian summer monsoon has also been widely studied (Zhang et al., 2025; Wood et al., 2023; He et al., 2022; Fleitmann et al., 2003; Gupta et al., 2003).

Compared to the 8.2 ka event, other early-Holocene climate events, such as the 9.2 ka event, receive less attention, and the dynamical causes of the 9.2 ka event are still unclear. Mao et al. (2016) proposed that the 9.2 ka event was influenced by a glacial meltwater pulse. This is similar to the physical mechanism of the 8.2 ka event, which suggests that the freshwater pulse inhibited the formation of the North Atlantic Deep

* Corresponding author at: School of Geography, Nanjing Normal University, Nanjing 210023, China.

E-mail address: lucy2012_2015@163.com (Y. Liang).

¹ The authors contributed equally to this work

Water (NADW), leading to weakened Atlantic Meridional Overturning Circulation (AMOC) and reduced heat transport. Some studies suggested that solar forcing was the main factor for this event because it can cause low-frequency decadal changes in global precipitation (Liu et al., 2018). Zhang et al. (2015) also linked monsoon weakening events during the early Holocene to solar activity changes. In contrast, Zhang et al. (2018) and Liang et al. (2020a) proposed a combination of external forcing and internal variability. They emphasized the significant weakening of the Asian monsoon at low and mid latitudes (Liang et al., 2020a; Zhang et al., 2018). This weakening is caused by an abrupt decrease in solar radiation, which may be coupled with the AMOC weakening (Zhang et al., 2018). Whether the monsoon weakening during the 9.2 ka event was triggered by external factors, such as solar activity, or by internal variability, such as the AMOC weakening, is still ambiguous. Therefore, more research is needed to determine the causes of the Asian monsoon weakening event at 9.2 ka BP.

In this study, we reconstruct the Asian summer monsoon evolution record with an average resolution of ~38 years from ~2332 to 9793 years before present based on $^{230}\text{Th}/\text{U}$ dating and stable isotope ($\delta^{13}\text{C}$ and $\delta^{18}\text{O}$) data from a stalagmite from Dongge Cave, Guizhou Province, southwestern China. We observe two significant weak monsoon events during the early Holocene (8.2 ka and 9.2 ka events) in the stalagmite record, and the abrupt monsoon events have remarkable similarities in the $\delta^{13}\text{C}$ and $\delta^{18}\text{O}$ records, with a one-to-one correspondence. The objectives of our study are: (1) to clarify the characteristics of Asian monsoon and environmental changes in southwestern China during the 9.2 ka event, and (2) to analyze the mechanisms of Asian monsoon weakening during the 9.2 ka event.

2. Materials and methods

The stalagmite sample (No. DD) was collected from Dongge Cave ($25^{\circ}17'\text{N}$, $108^{\circ}5'\text{E}$, 680 m above sea level), which is developed in the Carboniferous limestone (Liu et al., 2016). It is located 18 km southeast of Libo County in Guizhou Province, southwestern China, and it is strongly influenced by the Asian monsoon, characterized by warm, humid summers and cold, dry winters. The average annual precipitation near the cave is 1753 mm, most of which (80 %) occurs in the months with prevailing summer monsoon (May to October), while less precipitation (20 %) occurs in the months with prevailing winter monsoon (November to April). The average annual temperature and relative humidity in the cave are 15.6°C and greater than 90 %, respectively. The vegetation above this cave is mainly composed of evergreen broad-leaved plants (Liu et al., 2016).

Stalagmite sample DD is conical, with a total length of 200 mm and a diameter of ~30–80 mm (Fig. 1a). The sample was cut along its growth axis and then polished, and it is composed of transparent and pure calcite, according to the analytical results of XRD (Fig. S1). For stable isotope analyses, powdered subsamples weighing 90 μg were drilled from the polished surfaces along the growth axis. A total of 199 subsamples were drilled at 1-mm intervals. Carbon and oxygen isotope analyses were performed on a Finnigan MAT253 mass spectrometer coupled with a Kiel Carbonate Device at the School of Geography, Nanjing Normal University. All isotope values were reported in permil (‰) relative to the Vienna Pee Dee Belemnite (VPDB). Repeated measurements of the international standard (NBS19) indicated long-term reproducibility, with precisions better than 0.06 ‰ for $\delta^{18}\text{O}$ and 0.05 ‰ for $\delta^{13}\text{C}$ at the 1σ level.

For U—Th dating, a total of 12 powdered subsamples weighing 70 to 150 mg were drilled along the central growth axis. Nine of these subsamples were analyzed at the School of Geography, Nanjing Normal University, following chemical processes of uranium and thorium separation and purification as described in Shao et al. (2017). The uranium and thorium isotopic compositions were analyzed using a Neptune multi-collector inductively coupled plasma mass spectrometer (MC-ICP-MS). And $^{230}\text{Th}/\text{U}$ ages were obtained using an interactive program in

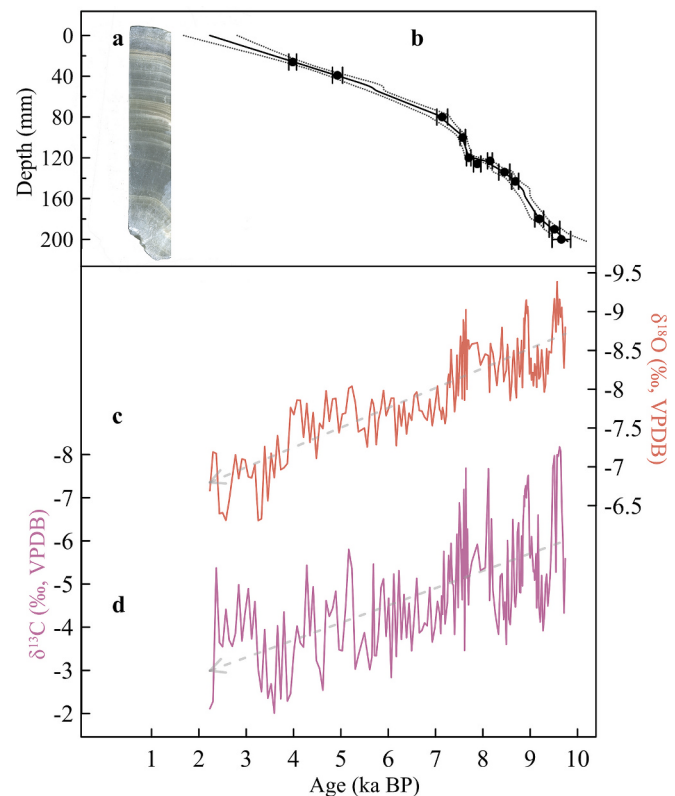


Fig. 1. Results of stalagmite DD. (a) Polished profile of DD sample. (b) Age vs. depth plot, black dots and error bars indicate $^{230}\text{Th}/\text{U}$ age and dating errors. (c) $\delta^{18}\text{O}$ and (d) $\delta^{13}\text{C}$ records of DD.

Nanjing Normal University (Shao et al., 2019). Three dating results marked with asterisks in Table 1 were processed and obtained at the Isotope Laboratory, Xi'an Jiaotong University. We followed chemistry procedures to separate uranium and thorium for dating (Edwards et al., 1987/88), and the separated solutions were then measured on the MC-ICP-MS, following similar procedures as described in Shen et al. (2012) and Cheng et al. (2013). The correction for the initial $^{230}\text{Th}/^{232}\text{Th}$ is $4.4 \pm 2.2 \times 10^{-6}$. All of the speleothem ages are in stratigraphic order with 2σ analytical errors.

3. Results

3.1. Chronology

A total of twelve $^{230}\text{Th}/\text{U}$ dating points were obtained for stalagmite DD. U and Th isotope concentrations and ratios, as well as $^{230}\text{Th}/\text{U}$ data, are shown in Table 1. These samples had ^{238}U concentrations ranging from 88.4 ± 0.03 to 141.1 ± 0.2 ppb (parts per billion) and ^{232}Th concentrations ranging from 46 ± 6 to 805 ± 7 ppt (parts per trillion). Due to the fact that most of the dates are arranged in stratigraphic order, we used the MOD AGE model (Hercman and Pawlak, 2012) to create the depth-age chronology for the stalagmite. We yield a growth period for the sample from ~2332 to 9793 a BP, with an average temporal resolution of ~38 years (Fig. 1b).

3.2. $\delta^{13}\text{C}$ and $\delta^{18}\text{O}$ sequences

Using a combination of $^{230}\text{Th}/\text{U}$ chronology and stable isotope data, we obtained $\delta^{13}\text{C}$ and $\delta^{18}\text{O}$ records of the stalagmite DD (Fig. 1c, d). The $\delta^{18}\text{O}$ values of DD range from -9.4 ‰ to -6.3 ‰, with an average of -8.0 ‰ and an amplitude of 3.1 ‰. The $\delta^{13}\text{C}$ values of DD varied from -8.2 ‰ to -2.0 ‰, with an average of -4.9 ‰ and a variation of 6.2 ‰.

Table 1²³⁰Th/U dating results for stalagmite DD from Dongge Cave.

Sample	²³⁸ U (ppb)	²³² Th (ppt)	²³⁰ Th / ²³² Th (atomic x10 ⁻⁶)	$\delta^{234}\text{U}^*$ (measured)	²³⁰ Th / ²³⁸ U (activity)	²³⁰ Th Age (yr) (uncorrected)	$\delta^{234}\text{U}_{\text{initial}}^{**}$	²³⁰ Th Age (yr BP) ^{***} (corrected)
Number								
DD-26	96.6 ± 0.12	106 ± 2	520.85 ± 15.09	-61.3 ± 1.4	0.0345 ± 0.0006	4090 ± 78	-62 ± 1.5	3982 ± 82
DD-39	120.4 ± 0.03	794 ± 7	20.43 ± 0.22	-54.4 ± 1.1	0.0441 ± 0.0003	5132 ± 33	-55 ± 1.1	4929 ± 107
DD-80	117.6 ± 0.03	805 ± 7	27.46 ± 0.27	-65.5 ± 1.1	0.0615 ± 0.0003	7356 ± 40	-67 ± 1.1	7142 ± 114
DD-100	90.8 ± 0.02	157 ± 5	113.47 ± 3.93	-57.3 ± 1.3	0.0643 ± 0.0004	7628 ± 50	-59 ± 1.4	7574 ± 57
DD-120	88.4 ± 0.03	46 ± 6	381.20 ± 45.89	-62.9 ± 0.9	0.0646 ± 0.0004	7718 ± 46	-64 ± 0.9	7701 ± 46
DD-123*	110.3 ± 0.2	54 ± 1	2280 ± 52	-62.2 ± 1.3	0.0682 ± 0.0004	8240 ± 49	-64 ± 1	8149 ± 50
DD-126*	113.7 ± 0.2	256 ± 5	487 ± 10	-61.1 ± 1.6	0.0666 ± 0.0005	8025 ± 59	-62 ± 2	7880 ± 77
DD-134	97.1 ± 0.03	656 ± 6	32.42 ± 0.36	-68.9 ± 0.9	0.0717 ± 0.0004	8665 ± 49	-71 ± 0.9	8453 ± 117
DD-143	110.9 ± 0.03	386 ± 6	62.67 ± 1.00	-86.2 ± 0.9	0.0713 ± 0.0004	8795 ± 48	-88 ± 1.0	8684 ± 73
DD-180	106.8 ± 0.03	484 ± 6	50.93 ± 0.69	-85.6 ± 1.1	0.0755 ± 0.0004	9335 ± 57	-88 ± 1.1	9190 ± 92
DD-190*	129.1 ± 0.2	480 ± 10	355 ± 8	-60.1 ± 1.7	0.0800 ± 0.0006	9703 ± 76	-62 ± 2	9513 ± 112
DD-200	95.6 ± 0.13	728 ± 15	176.68 ± 3.93	-65.6 ± 1.4	0.0816 ± 0.0008	9970 ± 102	-67 ± 1.4	9659 ± 196

U decay constants: $\lambda_{238} = 1.55125 \times 10^{-10}$ (Jaffey et al., 1971) and $\lambda_{234} = 2.82206 \times 10^{-6}$ (Cheng et al., 2013). Th decay constant: $\lambda_{230} = 9.1705 \times 10^{-6}$ (Cheng et al., 2013).

* $\delta^{234}\text{U} = ([^{234}\text{U}/^{238}\text{U}]_{\text{activity}} - 1) \times 1000$. ** $\delta^{234}\text{U}_{\text{initial}}$ was calculated based on ²³⁰Th age (T), i.e., $\delta^{234}\text{U}_{\text{initial}} = \delta^{234}\text{U}_{\text{measured}} \times e^{\lambda^{234}\times T}$.

Corrected ²³⁰Th ages assume the initial ²³⁰Th/²³²Th atomic ratio of $(4.4 \pm 2.2) \times 10^{-6}$. Those are the values for a material at secular equilibrium, with the bulk earth ²³²Th/²³⁸U value of 3.8. The errors are arbitrarily assumed to be 50 %.

*** BP stands for “Before Present” where the “Present” is defined as the year 1950 CE.

The long-term evolution of the $\delta^{13}\text{C}$ and $\delta^{18}\text{O}$ records is consistent from 9.7 to 2.1 ka BP, showing an overall positive trend (Fig. 1c, d) and a high positive correlation ($r = 0.78$, $n = 199$). Several centennial-scale variations are superimposed on the long-term trend of the $\delta^{13}\text{C}$ and $\delta^{18}\text{O}$ records. We did a Hendy test to sample DD to check whether it was influenced by kinetic fractionation during deposition (Hendy, 1971). Results show coeval $\delta^{18}\text{O}$ and $\delta^{13}\text{C}$ data on five different depths and the absence of a relationship between $\delta^{18}\text{O}$ and $\delta^{13}\text{C}$ values, indicating insignificant kinetic fractionation (Fig. S2). Therefore, $\delta^{18}\text{O}$ and $\delta^{13}\text{C}$ values in sample DD should likely reflect climatic and environmental changes.

4. Discussions

4.1. Imprints of the 8.2 ka and 9.2 ka events in the stalagmite records of Dongge Cave

In conjunction with records published in previous studies (Dykoski et al., 2005; Wang et al., 2005), we intend to reveal the patterns of three different stalagmites (DA, D4, and DD) from the same cave in response to the 8.2 and 9.2 ka events (Fig. 2). Due to the limited deposition period of the DA stalagmite, it misses the 9.2 ka event but captures the 8.2 ka event. The 8.2 ka event caused a large-amplitude positive shift in the DA $\delta^{18}\text{O}$ record, with an amplitude of ~0.8 ‰. Stalagmite D4 responds relatively weakly to the 8.2 ka event, but dramatically to the 9.2 ka event, with amplitudes of ~0.8 ‰ and ~1.3 ‰, respectively. Despite its low resolution, stalagmite DD records both centennial-scale events, with amplitudes of ~0.8 ‰ and ~1.2 ‰ for the 8.2 and 9.2 ka events, respectively. Quantitative calculations show that, although the three stalagmites exhibit significant differences in signal clarity for these two events, changes in their amplitudes were statistically similar; that is, ~0.8 ‰ for the 8.2 ka event and ~1.2 ‰ for the 9.2 ka event, as shown by black scales in Fig. 2. Besides, we find that the structure of the 8.2 ka event in three stalagmite $\delta^{18}\text{O}$ records is featured with a ‘W’ shape, similar to the findings displayed by Duan et al. (2024), while the structure of the 9.2 ka event is a ‘V’ shape (Fig. S3). This corroborates the significant regional characteristics of centennial-scale abrupt climatic events and provides key evidence to understand the complexity of cave hydrological processes and their recording of climatic signals.

For both the 8.2 ka and 9.2 ka events, the $\delta^{13}\text{C}$ and $\delta^{18}\text{O}$ records of sample DD are remarkably similar, with one-to-one correspondence of positive shifts. Interestingly, the $\delta^{13}\text{C}$ record of DD shows a clear, large-amplitude and positively-biased response to both the 8.2 ka and 9.2 ka

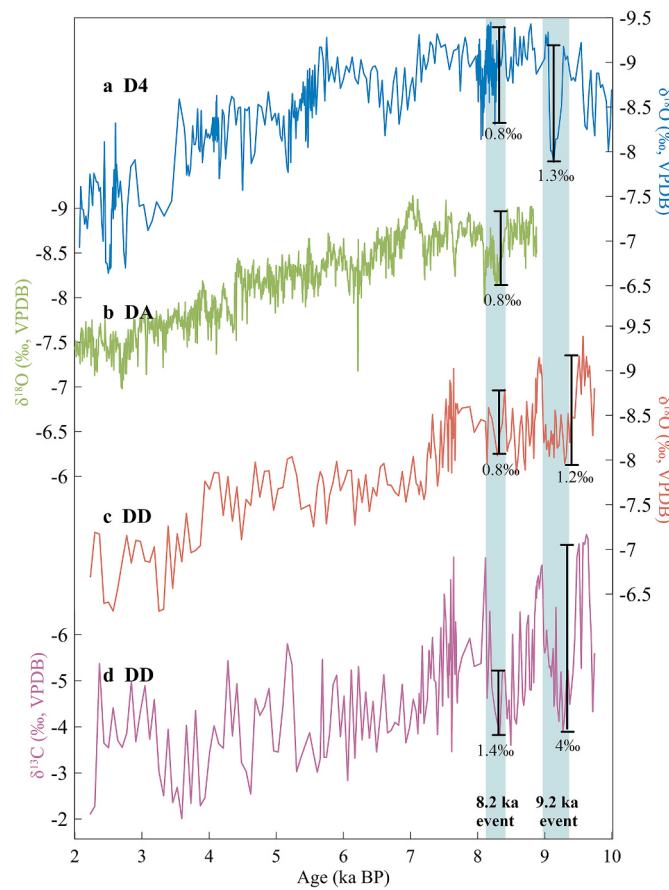


Fig. 2. Comparison of stalagmite records from Dongge Cave. The $\delta^{18}\text{O}$ records from (a) D4 (Dykoski et al., 2005), DA (Wang et al., 2005) and DD (this study). (d) The $\delta^{13}\text{C}$ record of sample DD (this study). Green bars indicate 8.2 ka and 9.2 ka events. Amplitudes of 8.2 ka and 9.2 ka events are indicated by black lines, with numbers aside. (For interpretation of the references to colour in this figure legend, the reader is referred to the web version of this article.)

events, with an amplitude of ~1.4 ‰ for the 8.2 ka event and ~4.0 ‰ for the 9.2 ka event (Fig. 2d). The carbon isotope composition of stalagmites is mainly derived from the composition of soil CO₂, biological processes (e.g., plant root respiration, microbial oxidation of organic

residues, etc.), vegetation types (C3 or C4 plants), and biomass production or soil respiration (Lechleitner et al., 2021; Genty et al., 2003). Cave stalagmite $\delta^{13}\text{C}$ is complexly affected by external conditions (e.g., climate, vegetation, etc.) and depositional processes (e.g., cave ventilation, prior calcite precipitation (PCP), etc.), and can provide important information on climate and environmental change (Fohlmeister et al., 2020; Fairchild et al., 2006; McDermott, 2004). Studies also show that changes in stalagmite $\delta^{13}\text{C}$ are indicative of the density and/or composition of vegetation (C3/C4) above the cave, which in turn may vary with the regional hydroclimate (Fohlmeister et al., 2020; Genty et al., 2003). In general, in humid and warm climates, increased biological productivity leads to higher concentrations of ^{12}C -enriched CO_2 in the soils due to abundant vegetation and active microbial activity (Genty et al., 2003). Subsequently, the ^{12}C -enriched CO_2 is transferred and deposited into secondary carbonate calcite, resulting in the formation of low-valued calcite $\delta^{13}\text{C}$ (Genty et al., 2003). On the contrary, under cold and dry climate conditions, decreased vegetation cover and biological productivity lead to positive shifts in calcite $\delta^{13}\text{C}$ (Genty et al., 2003). Previous studies from Dongge Cave show that calcite $\delta^{13}\text{C}$ from this cave can represent changes in C3/C4 vegetation ratio and soil processes above the cave (Zhang et al., 2004, 2006). Besides, Liu et al. (2016) found strong coupling of centennial-scale changes in $\delta^{13}\text{C}$ and $\delta^{18}\text{O}$ records, indicating that shifts of the Asian monsoon could contribute to $\delta^{13}\text{C}$ changes through ways of the soil conditions, vegetation density, and biological activity. The amplification effect of ecosystem processes on calcite $\delta^{13}\text{C}$ in response to the climatic signals (Frappier et al., 2002) is also observed in previous Dongge Cave studies (Zhang et al., 2004, 2006; Liu et al., 2016), further supporting our finding of a larger amplitude in $\delta^{13}\text{C}$ changes relative to $\delta^{18}\text{O}$ records. Therefore, the significant positive bias exhibited by stalagmite DD $\delta^{13}\text{C}$ records during the 8.2 ka and 9.2 ka events points to substantial changes in the overlying ecosystems and karst systems of Dongge Cave during these events: e.g., reduced vegetation productivity (C3/C4 ratio changes), reduced soil respiration rates, or restricted microbial activity due to reduced soil moisture and precipitation.

Differences in the sensitivity of the stalagmite $\delta^{13}\text{C}$ and $\delta^{18}\text{O}$ to the 8.2 ka and 9.2 ka events may result from the complexity of the controls on the isotopic composition. On the seasonal timescale, different source regions of the precipitation, the pathways between the moisture source and the cave site, and condensation and evaporation processes can all contribute to the variabilities in rainfall oxygen isotopic content at Dongge Cave site, apart from the precipitation amount and temperature (Dayem et al., 2010). On longer timescales, such as during the Holocene and the Last Interglacial Period, the Dongge Cave $\delta^{18}\text{O}$ proxy is likely to reflect the Asian Summer Monsoon (ASM) intensity (Yuan et al., 2004; Dykoski et al., 2005; Wang et al., 2005; Wan et al., 2011). In general, there are two mechanisms affecting $\delta^{18}\text{O}$ on orbital and millennial timescales: changes in monsoon rainfall as a proportion of total annual rainfall and changes in rainfall between tropical sources and caves (Cheng et al., 2016; Yuan et al., 2004; Wang et al., 2001). The former is caused by changes in the seasonal migration of subtropical jets, and the latter involves changes in rainfall from the Pacific and Indian Oceans (Liang et al., 2020b). However, stalagmite $\delta^{13}\text{C}$ proxies are highly dependent on the overlying vegetation type (C3/C4), soil bioactivity, and their climate responses. Therefore, forced by abrupt climate events, vegetation photosynthesis and soil microbial processes can respond rapidly, and changes in carbon isotope fractionation are easily captured by stalagmites. The combination of strong $\delta^{13}\text{C}$ and weak $\delta^{18}\text{O}$ responses in the stalagmite DD record likely suggests that key ecological processes at the overlying surface of the caves were strongly perturbed during these abrupt climate events, whereas changes in the regional integrated precipitation were relatively subdued. The good correlation between $\delta^{13}\text{C}$ and $\delta^{18}\text{O}$ suggests that regional hydrological and wetness changes were mainly controlled by the large-scale summer monsoon circulation. The magnitude of $\delta^{13}\text{C}$ changes exceeded the $\delta^{18}\text{O}$ signal by a factor of 3 on the 9.2 ka events, possibly suggesting that ecosystems have an

amplifying effect on climate signals (Zhao et al., 2016; Frappier et al., 2002).

4.2. The hemispheric influence of the 9.2 ka event

In this study, the $\delta^{13}\text{C}$ and $\delta^{18}\text{O}$ records of our stalagmite DD are sensitively responsive to climate changes during the 9.2 ka event, especially the dramatic changes in the $\delta^{13}\text{C}$ record. In the monsoonal region of China, the 9.2 ka event is also recorded in other geological reconstructions. In northern China, both Li et al. (2020) and Dong et al. (2018) identified a weak monsoon event at around 9 ka BP, based on high-resolution $\delta^{18}\text{O}$ records of stalagmites from Zhenzhu Cave and

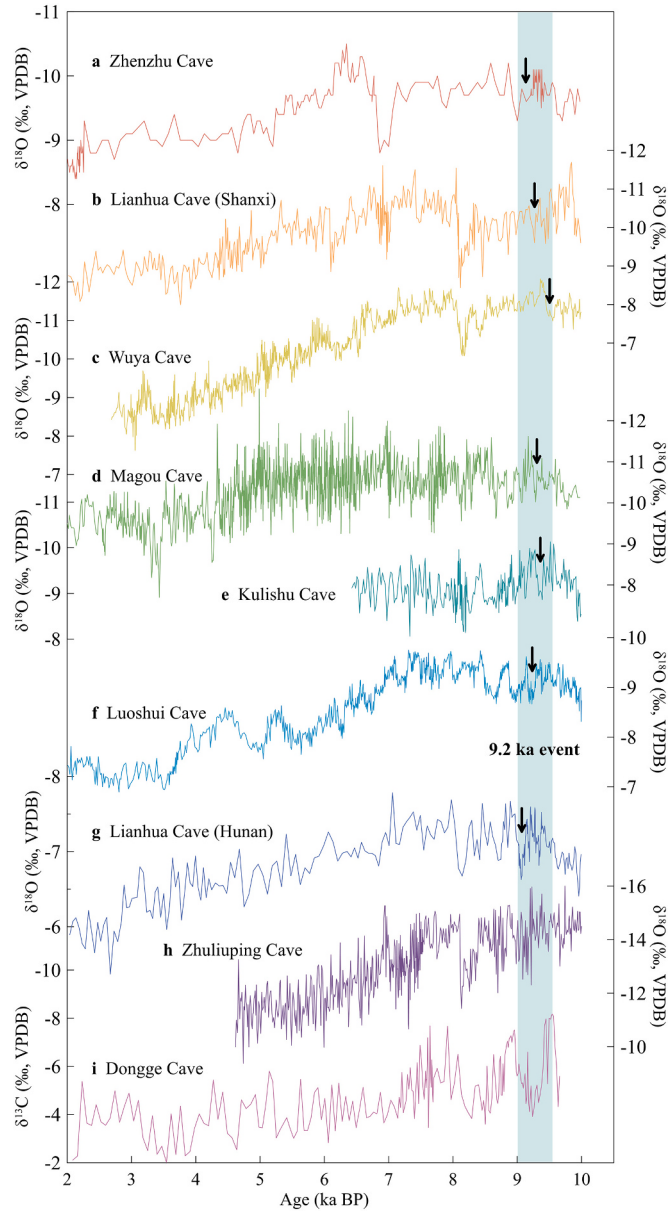


Fig. 3. Comparison of stalagmite records from the monsoonal region of China during the Holocene. The $\delta^{18}\text{O}$ records from (a) Zhenzhu Cave (Li et al., 2020), (b) Lianhua Cave in Shanxi Province (Dong et al., 2018), (c) Wuya Cave (Tan et al., 2020), (d) Magou Cave (Cai et al., 2021), (e) Kulishu Cave (Duan et al., 2021), (f) Luoshui Cave (Wang et al., 2022), (g) Lianhua Cave in Hunan Province (Zhang et al., 2016), (h) Zhuliuping Cave (Huang et al., 2016). (i) $\delta^{13}\text{C}$ record of sample DD from Dongge Cave (this study). Green bar and black arrows indicate the 9.2 ka event. (For interpretation of the references to colour in this figure legend, the reader is referred to the web version of this article.)

Lianhua Cave (Fig. 3a, b). Tan et al. (2020) reconstructed the highest-resolution record on the western Chinese Loess Plateau and identified eight weak monsoon events corresponding to the Bond events in the North Atlantic (centering at around 11.01, 10.52, 9.55, 8.15, 5.49, 3.90, 2.92, and 1.19 ka BP), and the 9.55-ka event is nearly coherent with the 9.2 ka event (Fig. 3c). The $\delta^{18}\text{O}$ values of stalagmites from Magou Cave also showed rapid positive excursions at 9.1 and 9.3 ka BP (Cai et al., 2021) (Fig. 3d). Furthermore, Duan et al. (2021) revealed rapid Asian summer monsoon changes during the early Holocene and identified five significant monsoon deteriorations at around 11.5, 11.0, 10.0, 9.4, and 8.2 ka BP by a stalagmite from Kulishu Cave (Fig. 3e). In central China, Wang et al. (2022) reconstructed the history of the ASM changes since 23.5 ka BP, which showed that a significant monsoon weakening event occurred near 9.2 ka BP (Fig. 3f). The LHD5 stalagmite $\delta^{18}\text{O}$ data from Lianhua Cave, Hunan Province, is used to reconstruct the Asian monsoon evolution during the Holocene, and six weak monsoon events centered at around 11.5, 10.4, 10, 9.1, 8.7, and 8.1 ka BP are identified (Zhang et al., 2016) (Fig. 3g). In southwestern China, Huang et al. (2016) identified four centennial-scale weak monsoon events in the early Holocene at 11.2, 10.8, 9.1, and 8.2 ka BP based on high-resolution isotope records of stalagmites from Zhiliuping Cave (Fig. 3h).

Furthermore, by analyzing peat sediments from Dajiuju Lake Basin in Shennongjia, central China, Zhang et al. (2018) combined geochemical indicators (e.g., total organic carbon (TOC), total nitrogen (TN), Al, Ti, Rb/Sr ratio, $\delta^{13}\text{C}$) and pollen records, and found that at ~9.2 ka BP, the TOC and TN contents of Dajiuju Lake peat sediments decreased dramatically, while Al and Ti contents increased significantly, indicating an interruption of peat development and a weakening of chemical weathering intensity. They also emphasized that the 9.2 ka event could have constituted the strongest abrupt collapse of the Asian monsoon system during the entire Holocene (Fig. 4a) (Zhang et al., 2018). You et al. (2025) quantitatively reconstructed mean annual precipitation variations based on the high-resolution multi-proxy analyses of cores from Bohai Bay, and they identified a significant monsoon weakening event surrounding 9.4 ka BP. This event was manifested by a decrease in precipitation of about 200 mm (minimum 444 mm), a sharp decrease in trees (e.g., *Quercus* spp.), and an expansion of herbs (You et al., 2025). The summer monsoon index (SMI) from Qinghai Lake decreased since 9.5 ka BP, with the minimum value occurring at around 9.2 ka BP, indicating a sharp decrease in the intensity of the Asian summer monsoon (An et al., 2012). The difference in $\delta^{13}\text{C}$ values between C₃₁ and C₂₉ n-alkanes from Huguangyan Maar Lake, as a surrogate for ASM intensity, also indicates a sharp weakening of the ASM intensity around 9.2 ka BP (Jia et al., 2015).

Other geological records around the globe, at least in the northern hemisphere, also captured the 9.2 ka event, portraying the internal structure and characteristics of this event. Rasmussen et al. (2007) identified a significant high-latitude cooling near 9.3 ka BP based on three ice cores from Greenland (DYE-3, GRIP, and NGRIP), with a duration of 40–100 years, reflecting significant fluctuation in response to the 9.2 ka event in the North Atlantic (Fig. 4 b–d). In central Europe, oxygen isotope sequences of deep-water ostracod shells from Lake Ammersee also show evidence of a pronounced cold event at 9.2 ka BP, with a temperature drop of 1.6 °C (Grafenstein et al., 1999) (Fig. 4e). Boch et al. (2009) revealed rapid climate changes in the early Holocene by stalagmites from the Katerloch Cave, Austria, and found that at ~9.1 ka BP, a significant negative oxygen isotope anomaly event lasted for 70–110 years with an amplitude of 1 ‰ (Fig. 4f). Spurk et al. (2002) examined the frequency of subfossil tree deposition in the Mainstem Valley region and observed a significant climate event at 9.2 ka BP, which is manifested by reduced deposition and deteriorating tree growth conditions. In North America, the high-resolution aquatic biomarkers from the Blood Pond revealed an abrupt cooling event near 9.2 ka BP, with the D/H ratios of behenic acid ($\delta\text{D}_{\text{BA}}$) shifts of up to 30 ‰, corresponding to a drop in precipitation-weighted temperature (PWT) of ~7 °C (Hou et al., 2012). Biosilica indicators from lake sediments in

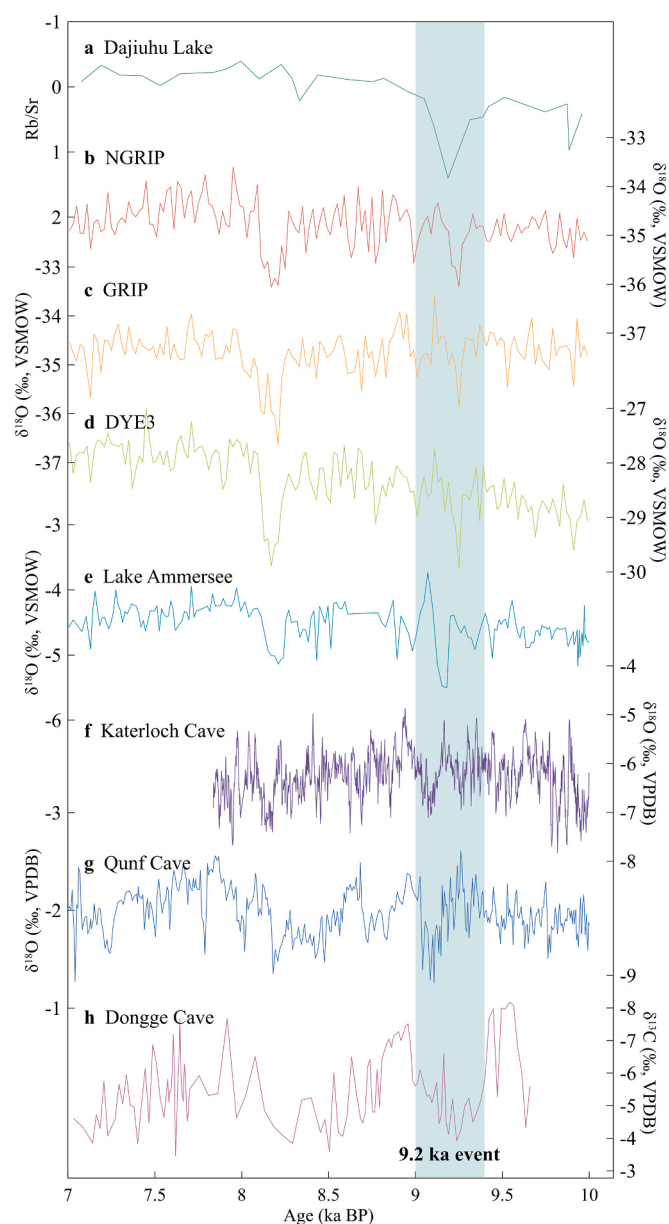


Fig. 4. The 9.2 ka event in different geological records. (a) Rb/Sr ratios of peat from Dajiuju Lake (Zhang et al., 2018). Greenland ice-core $\delta^{18}\text{O}$ records from (b) NGRIP, (c) GRIP and (d) DYE-3 (Rasmussen et al., 2007). (e) The $\delta^{18}\text{O}$ record from Lake Ammersee (Grafenstein et al., 1999). (f) The $\delta^{18}\text{O}$ record from Katerloch Cave (Boch et al., 2009). (g) The $\delta^{18}\text{O}$ record from Qunf Cave (Fleitmann et al., 2003). (h) The $\delta^{13}\text{C}$ record from sample DD (this study). The green bar indicates the 9.2 ka event. (For interpretation of the references to colour in this figure legend, the reader is referred to the web version of this article.)

southwest Alaska also show significant century-scale fluctuations in lake-phase productivity and terrestrial vegetation at 9.2 ka BP (Hu et al., 2003). Based on high-resolution lake records from southeastern Massachusetts, Newby et al. (2009) revealed that the 9.2 ka cooling event caused changes in sediment phases and an increase in grain size, indicating drying conditions in that region. In Asia, the Indian monsoon precipitation changes reconstructed by analyzing the high-resolution $\delta^{18}\text{O}$ record of stalagmites from the Qunf Cave in southern Oman show that the monsoon precipitation changes are consistent with Greenland temperature fluctuations during the 9.2 ka event (Fleitmann et al., 2003) (Fig. 4g). Gupta et al. (2003) analyzed changes in the abundance of planktonic foraminifera, a proxy for the strength of the

Indian summer monsoon, from ODP 723 A, and found a significant monsoon collapse event around 9.2 ka BP.

By comparing the stalagmite $\delta^{18}\text{O}$ record in the monsoonal region of China with other global geologic records, it is found that the 9.2 ka event has a significant impact on the North Atlantic, North America, Eurasia, and the Asian monsoon region. All these records collectively corroborate the hemispheric signature of the abrupt 9.2 ka event, mainly displaying a drying and cooling condition in the Northern Hemisphere. Although the 9.2 ka event is recognized in these studies, the onset of the event in these records are different, and the possible reasons include: (1) errors in dating methods and resolution limitations, (2) time lags in the transmission of the solar radiation weakening signal to different regions through the atmospheric circulation, (3) differences of regional response in ASM and northern hemisphere solar insolation forcing coupling, and thermal forcing heterogeneity due to complex geographic configurations (Cai et al., 2010; Wang et al., 2003), (4) sensitive response to rapid southward retreat of the Intertropical Convergence Zone (ITCZ) at low latitudes (Tan, 2016; Wang et al., 2003).

4.3. Mechanism for Asian Summer Monsoon changes during the 9.2 ka event

Our stalagmite DD captures two abrupt climate events that occurred at around 8.2 and 9.2 ka BP, and the 9.2 ka event shows a more intensive response, with $\delta^{13}\text{C}$ and $\delta^{18}\text{O}$ exhibiting dramatic positive shifts, indicating a dramatic monsoon collapse and environmental deterioration. Changes in freshwater inputs to the deepwater North Atlantic are considered to be an important driver of the abrupt ASM weakening events at millennial timescales in the early Holocene (Cheng et al., 2012; Pausata et al., 2011; Yu et al., 2010; Wang et al., 2008; Gupta et al., 2003). A widely accepted view is that the 9.2 ka and 8.2 ka climatic events share the same causal mechanism, i.e., a large influx of freshwater into the North Atlantic affects the thermohaline circulation system, leading to a slowdown of the AMOC. The correlation between the ASM weakening and the North Atlantic ice rafted debris record before and after the 9.2 ka BP validates that changes in the North Atlantic could affect the ASM (Bond et al., 2001) (Fig. 5a). The North Atlantic freshwater input can reduce the North Atlantic thermohaline circulation, which weakens the ocean heat transport capacity between the two hemispheres, causing cooling in the boreal high latitudes and warming in the tropics and the Southern Hemisphere. The heat balance between the Northern and Southern Hemispheres will be disrupted, leading to the southward shift of the ITCZ, the weakening of the ASM and a significant decrease in precipitation across the East Asia (Fleitmann et al., 2008; Ellison et al., 2006; Dahl et al., 2005; Wang et al., 2005; Gupta et al., 2003; Clark et al., 2002), which is supported by model simulations (Yu et al., 2009; Broccoli et al., 2006; Chiang and Bitz, 2005; Haug et al., 2001).

However, this observation does not explain the fact that the 9.2 ka event in Dongge Cave records has a more intense amplitude than the 8.2 ka event. In Dongge $\delta^{18}\text{O}$ records, the 8.2 ka event has an average amplitude of $\sim 0.8\text{‰}$, and the 9.2 ka event has a mean amplitude of $\sim 1.2\text{‰}$. In our DD $\delta^{13}\text{C}$ record, the amplitude is $\sim 1.4\text{‰}$ for the 8.2 ka event and $\sim 4\text{‰}$ for the 9.2 ka event. However, the North Atlantic ice-rafted debris record shows more accumulated freshwater influx into the North Atlantic during the 8.2 ka event than during the 9.2 ka event. And the melting of the Laurentide Ice Sheet was very fast during the 8.2 ka event, while it was slow during the 9.2 ka event (Ullman et al., 2016). Therefore, we suggest that the freshwater input only partially explains the 9.2 ka event, and changes in solar radiation could also play a role in monsoon changes at low latitudes in addition to the high-latitude forcing in the North Atlantic (Yan et al., 2015; Liu et al., 2009). When the effective solar radiation increases, the warming over the Asian continent is much stronger than that over the neighboring oceans, thus enhancing the thermal difference between land and sea. This increased thermal difference further enhances the air pressure difference between the

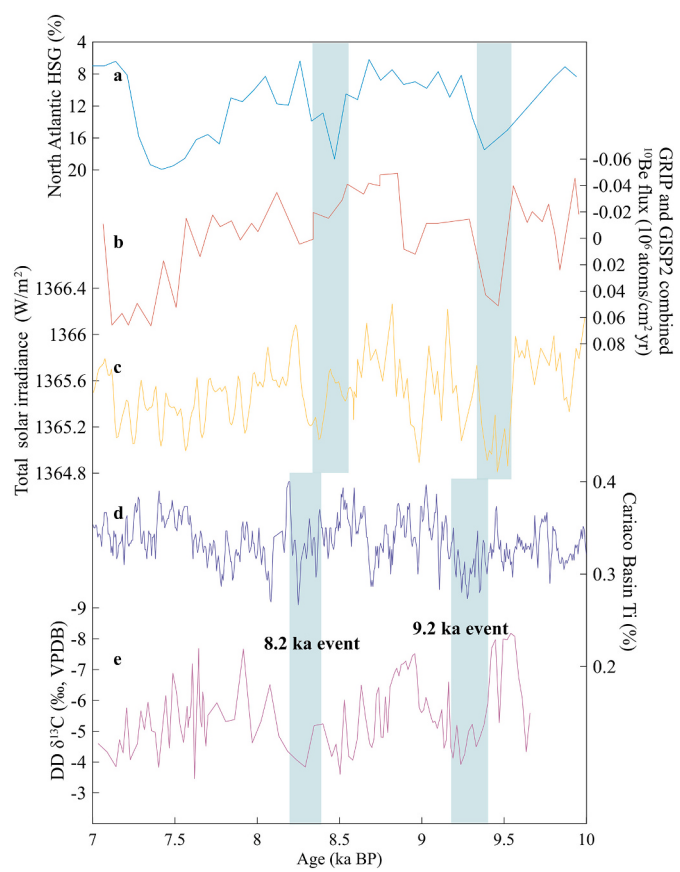


Fig. 5. Comparison of geologic reconstructions during the 8.2 ka and 9.2 ka events. (a) Hematite staining granule (HSG) contents in the North Atlantic (Bond et al., 2001). (b) ^{10}Be flux combination from ice cores of GRIP and GISP2 (Muscheler et al., 2004). (c) Total solar irradiance (TSI) (W/m^2) (Vieira et al., 2011). (d) Ti content record of sediments from the Cariaco Basin (Haug et al., 2001). (e) The $\delta^{13}\text{C}$ record of DD sample from Dongge Cave (this study). Green bars indicate 8.2 ka and 9.2 ka events. (For interpretation of the references to colour in this figure legend, the reader is referred to the web version of this article.)

monsoonal regions and the surrounding ocean, thereby strengthening the monsoon circulation and the associated precipitation (Yan et al., 2015; Liu et al., 2009). It is noteworthy that the weakening of solar radiation around 9.2 ka BP is relatively stronger than that around 8.2 ka BP (Fig. 5b, c). Reduced total solar irradiance (TSI) leads to a weakening of the AMOC, and the ITCZ moves southward through oceanic regimes, resulting in a weakening of the ASM (Fleitmann et al., 2007; Broccoli et al., 2006; Wang et al., 2005). Sedimentary Ti content records from the low-latitude Cariaco Basin also show significant minima during the 9.2 ka event, indicating a coherent southward shift of the ITCZ (Haug et al., 2001) (Fig. 5d). Recent modeling studies of the ASM have shown the rapid development of the El Niño-like climate mode with the sharp decline in TSI, leading to a weakening of the ASM and a decrease in precipitation (Wang et al., 2023; Marchitto et al., 2010; Asmerom et al., 2007). In addition, there is a lag of 50–180 years between monsoon precipitation and the onset of TSI reduction and the El Niño phenomenon, indicating a delayed monsoon response (Wang et al., 2023).

In general, the sudden and large decrease in ASM around 9.2 ka BP may be related to changes in solar activity and the AMOC. The decrease of solar radiation would lead to a weakening of the ASM intensity by attenuating the monsoon water vapor transport from the tropical ocean to the continent at low latitudes, whereas the weakening of the AMOC due to the freshwater inputs from the North Atlantic Ocean would lead to a weakening of the ASM through the high and low latitude

interactions and southward shift of the ITCZ. We therefore imply that the synergistic effect of solar activity and AMOC may be the dominant factor for the 9.2 ka event, whereas the 8.2 ka event is more dependent on the direct effect of freshwater input from the North Atlantic.

5. Conclusions

Based on 12 high-precision ^{230}Th dating data and 199 pairs of stable isotopes ($\delta^{13}\text{C}$ and $\delta^{18}\text{O}$) in a stalagmite DD from Dongge Cave, southwestern China, we reconstructed the Asian summer monsoon evolution and environment history from ~ 2332 to 9793 a BP, with an average temporal resolution of ~ 38 years. Our sample DD, together with published records from the same cave, all capture the 8.2 ka and 9.2 ka events. The absolute changing amplitudes of these two events show similarity in three different stalagmites, confirming the significant regional character of these abrupt climate events. In addition, the amplitude of the DD $\delta^{13}\text{C}$ record exceeds that of the $\delta^{18}\text{O}$ records by more than a factor of 3 during the 8.2 ka and 9.2 ka events, which may suggest that the ecological processes in the overlying surface of the cave deteriorated dramatically during both events. The centennial-scale significant monsoon weakening event recorded by our stalagmite sample DD, the 9.2 ka event, is also recorded in various reconstructions in the monsoonal region of China, as well as geological records from the North Atlantic, Europe, North America and South Asia, which verifies its hemispheric characteristics. By comparing with reconstructed records, our results indicate that the 8.2 ka and 9.2 ka events in the Asian monsoon region were controlled by different forcings. While the monsoon collapse related to the 8.2 ka event was mainly due to the freshwater and the AMOC weakening in the North Atlantic, the rapid decrease in the ASM around 9.2 ka BP is likely related to the AMOC weakening as well as the decline in solar activity.

CRediT authorship contribution statement

Chuntong He: Writing – review & editing, Writing – original draft, Investigation, Data curation. **Bin Zhao:** Writing – review & editing, Funding acquisition, Data curation. **Yongjin Wang:** Writing – review & editing, Resources, Funding acquisition. **Kan Zhao:** Writing – review & editing, Funding acquisition. **Shaohua Yang:** Writing – review & editing, Funding acquisition. **Qingfeng Shao:** Writing – review & editing, Data curation. **Hai Cheng:** Data curation. **Yijia Liang:** Writing – review & editing, Supervision, Funding acquisition.

Declaration of competing interest

The authors declare that they have no known competing financial interests or personal relationships that could have appeared to influence the work reported in this paper.

Data availability

The authors confirm that all data necessary for supporting the scientific findings of this paper have been provided.

Acknowledgement

This work was supported by National Key Research and Development Program of China (Grant No. 2023YFF0804700) and National Natural Science Foundation of China (Grant No. 42207505, 41931178 and 42071105), Natural Science Foundation of Jiangsu Province (BK20230707) and Postgraduate Research & Practice Innovation Program of Jiangsu Province (KYCX25_1982).

Appendix A. Supplementary data

Supplementary data to this article can be found online at <https://doi.org/10.1016/j.palaeo.2025.113271>.

<https://doi.org/10.1016/j.palaeo.2025.113271>.

References

- Alley, R., Agustsdottir, A., 2005. The 8k event: cause and consequences of a major holocene abrupt climate change. *Quat. Sci. Rev.* 24, 1123–1149. <https://doi.org/10.1016/j.quascirev.2004.12.004>.
- Alley, R.B., Mayewski, P.A., Sowers, T., Stuiver, M., Taylor, K.C., Clark, P.U., 1997. Holocene climatic instability: a prominent, widespread event 8200 yr ago. *Geology* 25, 483. [https://doi.org/10.1130/0091-7613\(1997\)025<0483:HCIAPW>2.3.CO;2](https://doi.org/10.1130/0091-7613(1997)025<0483:HCIAPW>2.3.CO;2).
- An, Z., Colman, S.M., Zhou, W., Li, Xiaoqiang, Brown, E.T., Jull, A.J.T., Cai, Y., Huang, Y., Lu, X., Chang, H., Song, Y., Sun, Y., Xu, H., Liu, W., Jin, Z., Liu, Xiaodong, Cheng, P., Liu, Y., Ai, L., Li, Xiangzhong, Liu, Xiuju, Yan, L., Shi, Z., Wang, X., Wu, F., Qiang, X., Dong, J., Lu, F., Xu, X., 2012. Interplay between the westerlies and asian monsoon recorded in Lake Qinghai sediments since 32 ka. *Sci. Rep.* 2, 619. <https://doi.org/10.1038/srep00619>.
- Asmerom, Y., Polyak, V., Burns, S., Rasmussen, J., 2007. Solar forcing of holocene climate: New insights from a speleothem record, southwestern United States. *Geology* 35, 1. <https://doi.org/10.1130/G22865A.1>.
- Barber, D.C., Dyke, A., Hillaire-Marcel, C., Jennings, A.E., Andrews, J.T., Kerwin, M.W., Bilodeau, G., McNeely, R., Southon, J., Morehead, M.D., Gagnon, J.-M., 1999. Forcing of the cold event of 8,200 years ago by catastrophic drainage of laurentide lakes. *Nature* 400, 344–348. <https://doi.org/10.1038/22504>.
- Boch, R., Spötl, C., Kramers, J., 2009. High-resolution isotope records of early holocene rapid climate change from two coeval stalagmites at katerloch cave, Austria. *Quat. Sci. Rev.* 28, 2527–2538. <https://doi.org/10.1016/j.quascirev.2009.05.015>.
- Bond, G., Showers, W., Cheseby, M., Lotti, R., Almasi, P., deMenocal, P., Priore, P., Cullen, H., Hajdas, I., Bonani, G., 1997. A pervasive millennial-scale cycle in North Atlantic holocene and glacial climates. *Science* 278, 1257–1266. <https://doi.org/10.1126/science.278.5341.1257>.
- Bond, G., Kromer, B., Beer, J., Muscheler, R., Evans, M.N., Showers, W., Hoffmann, S., Lotti-Bond, R., Hajdas, I., Bonani, G., 2001. Persistent solar influence on North Atlantic climate during the holocene. *Science* 294, 2130–2136. <https://doi.org/10.1126/science.1065680>.
- Broccoli, A.J., Dahl, K.A., Stouffer, R.J., 2006. Response of the ITCZ to northern hemisphere cooling. *Geophys. Res. Lett.* 33, 2005GL024546. <https://doi.org/10.1029/2005GL024546>.
- Cai, Y., Tan, L., Cheng, H., An, Z., Edwards, R.L., Kelly, M.J., Kong, X., Wang, X., 2010. The variation of summer monsoon precipitation in Central China since the last deglaciation. *Earth Planet. Sci. Lett.* 291, 21–31. <https://doi.org/10.1016/j.epsl.2009.12.039>.
- Cai, Y., Cheng, X., Ma, L., Mao, R., Breitenbach, S.F.M., Zhang, H., Xue, G., Cheng, H., Edwards, R.L., An, Z., 2021. Holocene variability of East Asian summer monsoon as viewed from the speleothem $\delta^{18}\text{O}$ records in Central China. *Earth Planet. Sci. Lett.* 558, 116758. <https://doi.org/10.1016/j.epsl.2021.116758>.
- Cheng, H., Sinha, A., Wang, X., Cruz, F.W., Edwards, R.L., 2012. The Global Paleomonsoon as seen through speleothem records from Asia and the Americas. *Clim. Dyn.* 39, 1045–1062. <https://doi.org/10.1007/s00382-012-1363-7>.
- Cheng, H., Edwards, R.L., Shen, C.-C., Polyak, V.J., Asmerom, Y., Woodhead, J.D., Hellstrom, J., Wang, Y., Kong, X., Spötl, C., Wang, X., Alexander, E.C., 2013. Improvements in ^{230}Th dating, ^{230}Th and ^{234}U half-life values, and U-Th isotopic measurements by multi-collector inductively coupled plasma mass spectrometry. *Earth Planet. Sci. Lett.* 371, 82–91. <https://doi.org/10.1016/j.epsl.2013.04.006>.
- Cheng, H., Edwards, R.L., Sinha, A., Spötl, C., Yi, L., Chen, S., Kelly, M., Kathayat, G., Wang, X., Li, X., Kong, X., Wang, Y., Ning, Y., Zhang, H., 2016. The asian monsoon over the past 640,000 years and ice age terminations. *Nature* 534, 640–646. <https://doi.org/10.1038/nature18591>.
- Chiang, J.C.H., Bitz, C.M., 2005. Influence of high latitude ice cover on the marine intertropical convergence zone. *Clim. Dyn.* 25, 477–496. <https://doi.org/10.1007/s00382-005-0040-5>.
- Clark, P.U., Pisias, N.G., Stocker, T.F., Weaver, A.J., 2002. The role of the thermohaline circulation in abrupt climate change. *Nature* 415, 863–869. <https://doi.org/10.1038/415863a>.
- Dahl, K.A., Broccoli, A.J., Stouffer, R.J., 2005. Assessing the role of North Atlantic freshwater forcing in millennial scale climate variability: a tropical Atlantic perspective. *Clim. Dyn.* 24, 325–346. <https://doi.org/10.1007/s00382-004-0499-5>.
- Dayem, K.E., Molnar, P., Battisti, D.S., Roe, G.H., 2010. Lessons learned from oxygen isotopes in modern precipitation applied to interpretation of speleothem records of paleoclimate from eastern Asia. *Earth Planet. Sci. Lett.* 295, 219–230. <https://doi.org/10.1016/j.epsl.2010.04.003>.
- Ding, Y., Chan, J.C.L., 2005. The East Asian summer monsoon: an overview. *Meteorog. Atmos. Phys.* 89, 117–142. <https://doi.org/10.1007/s00703-005-0125-z>.
- Dong, J., Shen, C.-C., Kong, X., Wu, C.-C., Hu, H.-M., Ren, H., Wang, Y., 2018. Rapid retreat of the east asian summer monsoon in the middle holocene and a millennial weak monsoon interval at 9 ka in northern China. *J. Asian Earth Sci.* 151, 31–39. <https://doi.org/10.1016/j.jseas.2017.10.016>.
- Duan, W., Ma, Z., Tan, M., Cheng, H., Edwards, R.L., Wen, X., Wang, X., Wang, L., 2021. Timing and structure of early-holocene climate anomalies inferred from north chinese stalagmite records. *Holocene* 31, 1777–1785. <https://doi.org/10.1177/09596836211033218>.
- Duan, P., Li, H., Ma, Z., Zhao, J., Dong, X., Sinha, A., Hu, P., Zhang, H., Ning, Y., Zhu, G., Cheng, H., 2024. A series of climate oscillations around 8.2 ka revealed through multi-proxy speleothem records from North China. *Clim. Past* 20, 1401–1414. <https://doi.org/10.5194/cp-20-1401-2024>.

- Dykoski, C.A., Edwards, R.L., Cheng, H., Yuan, D., Cai, Y., Zhang, M., Lin, Y., Qing, J., An, Z., Revenaugh, J., 2005. A high resolution absolute dated holocene and deglacial asian monsoon record from Dongge Cave, China. *Earth Planet. Sci. Lett.* <https://doi.org/10.1016/j.epsl.2005.01.036>.
- Edwards, L.R., Chen, J.H., Wassburg, G.J., 1987. ^{238}U – ^{234}U – ^{230}Th – ^{232}Th systematics and the precise measurement of time over the past 500,000 years. *Earth Planet. Sci. Lett.* 81, 175–192. [https://doi.org/10.1016/0012-821X\(87\)90154-3](https://doi.org/10.1016/0012-821X(87)90154-3).
- Ellison, C.R.W., Chapman, M.R., Hall, I.R., 2006. Surface and deep ocean interactions during the cold climate event 8200 years ago. *Science* 312, 1929–1932. <https://doi.org/10.1126/science.1127213>.
- Fairchild, I.J., Smith, C.L., Baker, A., Fuller, L., Spötl, C., Matthey, D., McDermott, F., 2006. Modification and preservation of environmental signals in speleothems. *Earth Sci. Rev.* 75, 105–153. <https://doi.org/10.1016/j.earscirev.2005.08.003>.
- Fleitmann, D., Burns, S.J., Mudelsee, M., Neff, U., Kramers, J., Mangini, A., Matter, A., 2003. Holocene forcing of the indian monsoon recorded in a stalagmite from southern Oman. *Science* 300, 1737–1739. <https://doi.org/10.1126/science.1083130>.
- Fleitmann, D., Burns, S.J., Mangini, A., Mudelsee, M., Kramers, J., Villa, I., Neff, U., Al-Subbary, A.A., Buettner, A., Hipppler, D., Matter, A., 2007. Holocene ITCZ and Indian monsoon dynamics recorded in stalagmites from Oman and Yemen (Socotra). *Quat. Sci. Rev.* 26, 170–188. <https://doi.org/10.1016/j.quascirev.2006.04.012>.
- Fleitmann, D., Mudelsee, M., Burns, S.J., Bradley, R.S., Kramers, J., Matter, A., 2008. Evidence for a widespread climatic anomaly at around 9.2 ka before present. *Paleoceanography* 23, 2007PA001519. <https://doi.org/10.1029/2007PA001519>.
- Fohlmeister, J., Voarintsoa, N.R.G., Lechleitner, F.A., Boyd, M., Brandstätter, S., Jacobson, M.J., Oster, L., 2020. Main controls on the stable carbon isotope composition of speleothems. *Geochim. Cosmochim. Acta* 279, 67–87. <https://doi.org/10.1016/j.gca.2020.03.042>.
- Frappier, A., Sahagian, D., González, L.A., Carpenter, S.J., 2002. El Niño events recorded by stalagmite carbon isotopes. *Science* 298, 565. <https://doi.org/10.1126/science.1076446>.
- Genty, D., Genty, D., Blamart, D., Ouahdi, R., Gilmour, M., Baker, A., Jouzel, J., Jouzel, J., Jouzel, Jean, Van-Exter, S., 2003. Precise dating of Dansgaard-Oeschger climate oscillations in western Europe from stalagmite data. *Nature* 421, 833–837. <https://doi.org/10.1038/nature01391>.
- Grafenstein, U.V., Erlenkeuser, H., Brauer, A., Jouzel, J., Johnsen, S.J., 1999. A mid-european decadal isotope-climate record from 15,500 to 5000 years B.P. *Science* 284, 1654–1657. <https://doi.org/10.1126/science.284.5420.1654>.
- Gupta, A.K., Anderson, D.M., Overpeck, J.T., 2003. Abrupt changes in the asian southwest monsoon during the holocene and their links to the North Atlantic Ocean. *Nature* 421, 354–357. <https://doi.org/10.1038/nature01340>.
- Haug, G.H., Hughen, K.A., Sigman, D.M., Peterson, L.C., Röhl, U., 2001. Southward Migration of the Intertropical Convergence Zone through the Holocene. *Science* 293, 1304–1308. <https://doi.org/10.1126/science.1059725>.
- He, P., Liu, J., Wang, B., Sun, W., 2022. Understanding global monsoon precipitation changes during the 8.2 ka event and the current warm period. *Palaeogeogr. Palaeoclimatol. Palaeoecol.* 586, 110757. <https://doi.org/10.1016/j.palaeo.2021.110757>.
- Hendy, C.H., 1971. The isotopic geochemistry of speleothems—I. The calculation of the effects of different modes of formation on the isotopic composition of speleothems and their applicability as palaeoclimatic indicators. *Geochim. Cosmochim. Ac.* 35, 801–824. [https://doi.org/10.1016/0016-7037\(71\)90127-X](https://doi.org/10.1016/0016-7037(71)90127-X).
- Hercman, H., Pawlak, J., 2012. MOD-AGE: An age-depth model construction algorithm. *Quat. Geochronol.* 12, 1–10. <https://doi.org/10.1016/j.quageo.2012.05.003>.
- Hou, J., Huang, Y., Shuman, B.N., Oswald, W.W., Foster, D.R., 2012. Abrupt cooling repeatedly punctuated early-holocene climate in eastern North America. *Holocene* 22, 525–529. <https://doi.org/10.1177/0959683611427329>.
- Hu, F.S., Kaufman, D., Yoneji, S., Nelson, D., Shemesh, A., Huang, Y., Tian, J., Bond, G., Clegg, B., Brown, T., 2003. Cyclic variation and solar forcing of holocene climate in the alaskan subarctic. *Science* 301, 1890–1893. <https://doi.org/10.1126/science.1088568>.
- Huang, W., Wang, Y., Cheng, H., Edwards, R.L., Shen, C.-C., Liu, D., Shao, Q., Deng, C., Zhang, Z., Wang, Q., 2016. Multi-scale holocene asian monsoon variability deduced from a twin-stalagmite record in southwestern China. *Quat. Res.* 86, 34–44. <https://doi.org/10.1016/j.yqres.2016.05.001>.
- Jaffey, A.H., Flynn, K.F., Glendenin, L.E., Bentley, W.C., Essling, A.M., 1971. Precision measurement of half-lives and specific activities of U 235 and U 238. *Phys. Rev. C* 4, 1889–1906. <https://doi.org/10.1103/PhysRevC.4.1889>.
- Jia, G., Bai, Y., Yang, X., Xie, L., Wei, G., Ouyang, T., Chu, G., Liu, Z., Peng, P., 2015. Biogeochemical evidence of holocene east asian summer and winter monsoon variability from a tropical maar lake in southern China. *Quat. Sci. Rev.* 111, 51–61. <https://doi.org/10.1016/j.quascirev.2015.01.002>.
- Johnsen, S.J., Dahl-Jensen, D., Gundestrup, N., Steffensen, J.P., Clausen, H.B., Miller, H., Masson-Delmotte, V., Sveinbjörnsdóttir, A.E., White, J., 2001. Oxygen isotope and palaeotemperature records from six Greenland ice-core stations: camp century, dye-3, GRIP, GISP2, renland and NorthGRIP. *J. Quat. Sci.* 16, 299–307. <https://doi.org/10.1002/jqs.622>.
- Kobashi, T., Menzies, L., Jeltsch-Thömmes, A., Vinther, B.M., Box, J.E., Muscheler, R., Nakaegawa, T., Pfister, P.L., Döring, M., Leuenberger, M., Wanner, H., Ohmura, A., 2017. Volcanic influence on centennial to millennial holocene Greenland temperature change. *Sci. Rep.* 7, 1441. <https://doi.org/10.1038/s41598-017-01451-7>.
- Lechleitner, F.A., Day, C.C., Kost, O., Wilhelm, M., Haghipour, N., Henderson, G.M., Stoll, H.M., 2021. Stalagmite carbon isotopes suggest deglacial increase in soil respiration in western Europe driven by temperature change. *Clim. Past* 17, 1903–1918. <https://doi.org/10.5194/cp-17-1903-2021>.
- Li, Y., Rao, Z., Xu, Q., Zhang, S., Liu, X., Wang, Z., Cheng, H., Edwards, R.L., Chen, F., 2020. Inter-relationship and environmental significance of stalagmite $\delta^{13}\text{C}$ and $\delta^{18}\text{O}$ records from Zhenzhu Cave, North China, over the last 130 ka. *Earth Planet. Sci. Lett.* 536, 116149. <https://doi.org/10.1016/j.epsl.2020.116149>.
- Liang, Q., Wu, J., Zhao, X., 2020a. Variability of Asian summer monsoon during 9.2 ka event recorded by a stalagmite from Luoshui cave, Hubei province Central China. *Quat. Sci. Rev.* 40, 945–958. <https://doi.org/10.11928/j.issn.1001-7410.2020.04.10> (in Chinese with English Abstract).
- Liang, Y., Zhao, K., Edwards, R.L., Wang, Y., Shao, Q., Zhang, Z., Zhao, B., Wang, Q., Cheng, H., Kong, X., 2020b. East Asian monsoon changes early in the last deglaciation and insights into the interpretation of oxygen isotope changes in the Chinese stalagmite record. *Quat. Sci. Rev.* 250, 106699. <https://doi.org/10.1016/j.quascirev.2020.106699>.
- Liu, J., Wang, B., Ding, Q., Kuang, X., Soon, W., Zorita, E., 2009. Centennial variations of the global monsoon precipitation in the last millennium: results from ECHO-G model. *J. Clim.* 22, 2356–2371. <https://doi.org/10.1175/2008JCLI2353.1>.
- Liu, D., Wang, Y., Cheng, H., Edwards, R.L., Kong, X., Li, T.-Y., 2016. Strong coupling of centennial-scale changes of Asian monsoon and soil processes derived from stalagmite $\delta^{18}\text{O}$ and $\delta^{13}\text{C}$ records, southern China. *Quat. Res.* 85, 333–346. <https://doi.org/10.1016/j.yqres.2016.02.008>.
- Liu, F., Zhao, T., Wang, B., Liu, J., Luo, W., 2018. Different global precipitation responses to solar, volcanic, and greenhouse gas forcings. *J. Geophys. Res. Atmos.* 123, 4060–4072. <https://doi.org/10.1029/2017JD027391>.
- Mao, R., Cai, Y., Ma, L., 2016. Early to mid-Holocene paleoclimatic changes recorded by the stalagmites from the Magou Cave Henan Province. *J. Earth Environm.* 3, 254–268. <https://doi.org/10.7515/JEE201603004> (in Chinese with English Abstract).
- Marchitto, T.M., Muscheler, R., Ortiz, J.D., Carriquiry, J.D., Van Geen, A., 2010. Dynamical response of the tropical pacific ocean to solar forcing during the early holocene. *Science* 330, 1378–1381. <https://doi.org/10.1126/science.1194887>.
- McDermott, F., 2004. Palaeo-climate reconstruction from stable isotope variations in speleothems: a review. *Quat. Sci. Rev.* 23, 901–918. <https://doi.org/10.1016/j.quascirev.2003.06.021>.
- McKay, N.P., Kaufman, D.S., Arcusa, S.H., Kulus, H.R., Edge, D.C., Erb, M.P., Hancock, C. L., Routson, C.C., Żarczyński, M., Marshall, L.P., Roberts, G.K., Telles, F., 2024. The 4.2 ka event is not remarkable in the context of holocene climate variability. *Nat. Commun.* 15, 6555. <https://doi.org/10.1038/s41467-024-50886-w>.
- Muscheler, R., Beer, J., Wagner, G., Laj, C., Kissel, C., Raisbeck, G.M., Yiou, F., Kubik, P. W., 2004. Changes in the carbon cycle during the last deglaciation as indicated by the comparison of 10Be and 14C records. *Earth Planet. Sci. Lett.* 219, 325–340. [https://doi.org/10.1016/S0012-821X\(03\)00722-2](https://doi.org/10.1016/S0012-821X(03)00722-2).
- Newby, P.E., Donnelly, J.P., Shuman, B.N., MacDonald, D., 2009. Evidence of centennial-scale drought from southeastern Massachusetts during the pleistocene/holocene transition. *Quat. Sci. Rev.* 28, 1675–1692. <https://doi.org/10.1016/j.jquascirev.2009.02.020>.
- Pausata, F.S.R., Battisti, D.S., Nisancioğlu, K.H., Bitz, C.M., 2011. Chinese stalagmite $\delta^{18}\text{O}$ controlled by changes in the Indian monsoon during a simulated Heinrich event. *Nat. Geosci.* 4, 474–480. <https://doi.org/10.1038/ngeo1169>.
- Rasmussen, S.O., Vinther, B.M., Clausen, H.B., Andersen, K.K., 2007. Early holocene climate oscillations recorded in three Greenland ice cores. *Quat. Sci. Rev.* 26, 1907–1914. <https://doi.org/10.1016/j.quascirev.2007.06.015>.
- Shao, Q.-F., Pons-Branchu, E., Zhu, Q.-P., Wang, W., Valladas, H., Fontugne, M., 2017. High precision U/th dating of the rock paintings at mt. Huashan, Guangxi, southern China. *Quat. Res.* 88, 1–13. <https://doi.org/10.1017/qua.2017.24>.
- Shao, Q.-F., Li, C.-H., Huang, M.-J., Liao, Z.-B., Arps, J., Huang, C.-Y., Chou, Y.-C., Kong, X.-G., 2019. Interactive programs of MC-ICPMS data processing for 230Th/U geochronology. *Quat. Geochronol.* 51, 43–52. <https://doi.org/10.1016/j.jquageo.2019.01.004>.
- Shen, C.-C., Wu, C.-C., Cheng, H., Lawrence Edwards, R., Hsieh, Y.-T., Gallet, S., Chang, C.-C., Li, T.-Y., Lam, D.D., Kano, A., Hori, M., Spötl, C., 2012. High-precision and high-resolution carbonate 230Th dating by MC-ICP-MS with SEM protocols. *Geochim. Cosmochim. Ac.* 99, 71–86. <https://doi.org/10.1016/j.gca.2012.09.018>.
- Spurk, M., Leuschner, H.H., Baillie, M.G.L., Briffa, K.R., Friedrich, M., 2002. Depositional frequency of german subfossil oaks: climatically and non-climatically induced fluctuations in the holocene. *Holocene* 12, 707–715. <https://doi.org/10.1191/0959683602hl583rp>.
- Stager, J.C., Mayewski, P.A., 1997. Abrupt early to Mid-Holocene Climatic transition Registered at the Equator and the Poles. *Science* 276, 1834–1836. <https://doi.org/10.1126/science.276.5320.1834>.
- Tan, M., 2016. Circulation background of climate patterns in the past millennium: uncertainty analysis and re-reconstruction of ENSO-like state. *Sci. China Earth Sci.* 59, 1225–1241. <https://doi.org/10.1007/s11430-015-5256-6>.
- Tan, L., Li, Y., Wang, X., Cai, Y., Lin, F., Cheng, H., Ma, L., Sinha, A., Edwards, R.L., 2020. Holocene monsoon change and abrupt events on the western chinese loess plateau as revealed by accurately dated stalagmites. *Geophys. Res. Lett.* 47. <https://doi.org/10.1029/2020GL090273> e2020GL090273.
- Ullman, D.J., Carlson, A.E., Hostetler, S.W., Clark, P.U., Cuzzone, J., Milne, G.A., Winsor, K., Caffee, M., 2016. Final Laurentide ice-sheet deglaciation and Holocene climate-sea level change. *Quat. Sci. Rev.* 152, 49–59. <https://doi.org/10.1016/j.jquascirev.2016.09.014>.
- Vieira, L.E.A., Solanki, S.K., Krivova, N.A., Usoskin, I., 2011. Evolution of the solar irradiance during the holocene. *Astron. Astrophys.* 531, A6. <https://doi.org/10.1051/0004-6361/201015843>.
- Wan, N., Chung, W., Li, H.-C., Lin, H., Ku, T.-L., Shen, C.-C., Yuan, D., Zhang, M., Lin, Y., 2011. Comparison of speleothem $\delta^{18}\text{O}$ records from eastern China with solar insolation, ice core and marine records: Similarities and discrepancies on different

- time scales. *J. Asian Earth Sci.* 40, 1151–1163. <https://doi.org/10.1016/j.jeas.2010.06.010>.
- Wang, Y., Cheng, H., Edwards, R. Lawrence, Richard Lawrence, An, Z., Wu, J., Shen, C.-C., Dorale, J.A., 2001. A High-Resolution Absolute-Dated late Pleistocene Monsoon Record from Hulu Cave, China. *Science* 294, 2345–2348. <https://doi.org/10.1126/science.1064618>.
- Wang, B., Clemens, S.C., Liu, P., 2003. Contrasting the Indian and East Asian monsoons: implications on geologic timescales. *Mar. Geol.* 201, 5–21. [https://doi.org/10.1016/S0025-3227\(03\)00196-8](https://doi.org/10.1016/S0025-3227(03)00196-8).
- Wang, Y., Cheng, H., Edwards, R.L., He, Y., Kong, X., An, Z., Wu, J., Kelly, M.J., Dykoski, C.A., Li, X., 2005. The Holocene Asian Monsoon: Links to Solar changes and North Atlantic climate. *Science* 308, 854–857. <https://doi.org/10.1126/science.1106296>.
- Wang, Y., Cheng, H., Edwards, R.L., Kong, X., Shao, X., Chen, S., Wu, J., Jiang, X., Wang, X., An, Z., 2008. Millennial- and orbital-scale changes in the East Asian monsoon over the past 224,000 years. *Nature* 451, 1090–1093. <https://doi.org/10.1038/nature06692>.
- Wang, B., Xiang, B., Lee, J.-Y., 2013. Subtropical high predictability establishes a promising way for monsoon and tropical storm predictions. *Proc. Natl. Acad. Sci.* 110, 2718–2722. <https://doi.org/10.1073/pnas.1214626110>.
- Wang, Z., Chen, S., Wang, Y., Zhao, K., Liang, Y., Cheng, H., Shao, Q., Wang, X., Zhang, J., Wang, Q., Zhai, X., Edwards, R.L., 2022. A high-resolution stalagmite record from luoshui cave, Central China over the past 23.5 kyr. *Quat. Sci. Rev.* 282, 107443. <https://doi.org/10.1016/j.quascirev.2022.107443>.
- Wang, J., Sun, W., Liu, J., Ning, L., Yan, M., Chen, D., Ma, Y., 2023. Impact of centennial-scale solar activity reduction on the weakened asian monsoon event at 9.2 ka BP. *Palaeogeogr. Palaeoclimatol. Palaeoecol.* 628, 111771. <https://doi.org/10.1016/j.palaeo.2023.111771>.
- Wood, C.T., Johnson, K.R., Lewis Lindsey, E., Wright, K., Wang, J.K., Borsato, A., Griffiths, M.L., Mason, A., Henderson, G.M., Setera, J.B., Frisia, S., Keopanhyia, S., White, J.C., 2023. High-resolution, multiproxy speleothem record of the 8.2 ka event from mainland Southeast Asia. *Paleoceanogr. Paleoclimatol.* 38. <https://doi.org/10.1029/2023PA004675> e2023PA004675.
- Yan, H., Wei, W., Soon, W., An, Z., Zhou, W., Liu, Z., Wang, Y., Carter, R.M., 2015. Dynamics of the intertropical convergence zone over the western Pacific during the Little Ice Age. *Nat. Geosci.* 8, 315–320. <https://doi.org/10.1038/ngeo2375>.
- You, H., Yang, S., Li, Y., Zhang, S., Zhang, Z., Ma, L., Shi, J., Wang, Y., Zhang, X., Yang, Y., 2025. Characteristics and driving mechanisms of early Holocene weakened monsoon events: evidence from northern bohai bay, China. *Palaeogeogr. Palaeoclimatol. Palaeoecol.* 657, 112613. <https://doi.org/10.1016/j.palaeo.2024.112613>.
- Yu, L., Gao, Y., Wang, H., Guo, D., Li, S., 2009. The responses of east asian summer monsoon to the North Atlantic meridional overturning circulation in an enhanced freshwater input simulation. *Sci. Bull.* 54, 4724–4732. <https://doi.org/10.1007/s11434-009-0720-3>.
- Yu, S.-Y., Colman, S.M., Lowell, T.V., Milne, G.A., Fisher, T.G., Breckenridge, A., Boyd, M., Teller, J.T., 2010. Freshwater outburst from lake superior as a trigger for the cold event 9300 years ago. *Science* 328, 1262–1266. <https://doi.org/10.1126/science.1187860>.
- Yuan, D., Yuan, D., Cheng, H., Edwards, R.L., Dykoski, C.A., Kelly, M.J., Zhang, M., Qing, J., Lin, Y., Wang, Y., Wu, J., Dorale, J.A., An, Z., Cai, Y., 2004. Timing, Duration, and Transitions of the last Interglacial Asian Monsoon. *Science* 304, 575–578. <https://doi.org/10.1126/science.1091220>.
- Zhang, M., Tan, J., Wang, H., Feng, Y., Yang, Y., Zhu, X., 2004. The Cooling events from Stalagmite Records during the Middle and late Holocene in Southwest China. *Carsolog. Sin.* 7, 283–289 (in Chinese with English Abstract).
- Zhang, M., Zhu, X., Tan, J., Zhang, C., Luo, G., Yang, Y., 2006. Study on $\delta^{13}\text{C}$ Isotope Records from Stalagmites. *Guangxi Sci.* 5 (48–51), 57 (in Chinese with English Abstract).
- Zhang, Y., Yang, Y., Yang, X., Yin, J., 2015. Early Holocene Monsoon Evolution of High-resolution Stalagmite $\delta^{18}\text{O}$ Records: in Henan Laomu Cave. *Act. Sedimentolog. Sinic.* 33, 134–141. <https://doi.org/10.14027/j.cnki.cjxb.2015.01.014> (in Chinese with English Abstract).
- Zhang, H., Yin, J., Cheng, H., 2016. Discussion about the Mechanism of the Weak Summer Monsoon events during the early Holocene: a case study of precisely dated stalagmite record from Lianhua Cave, Hunan province. *China. Act. Sedimentolog. Sinic* 34, 281–291 (in Chinese with English Abstract).
- Zhang, W., Yan, H., Dodson, J., Cheng, P., Liu, C., Li, J., Lu, F., Zhou, W., An, Z., 2018. The 9.2 ka event in asian summer monsoon area: the strongest millennial scale collapse of the monsoon during the holocene. *Clim. Dyn.* 50, 2767–2782. <https://doi.org/10.1007/s00382-017-3770-2>.
- Zhang, X., Zhang, H., Zhang, R., Wang, J., Wang, M., Liang, Z., He, M., Wei, R., Cheng, H., 2025. Spatiotemporal pattern of the East Asian monsoon hydroclimate during the 8.2 ka event inferred from a new speleothem multi-proxy record from SE China. *Quat. Sci. Rev.* 349, 109141. <https://doi.org/10.1016/j.quascirev.2024.109141>.
- Zhao, K., Wang, Y., Edwards, R.L., Cheng, H., Liu, D., Kong, X., Ning, Y., 2016. Contribution of ENSO variability to the east asian summer monsoon in the late holocene. *Palaeogeogr. Palaeoclimatol. Palaeoecol.* 449, 510–519. <https://doi.org/10.1016/j.palaeo.2016.02.044>.